

## Mariner 9 Ultraviolet Spectrometer Experiment: Pressure-Altitude Measurements on Mars

C. W. HORD

*Department of Astro-Geophysics and Laboratory for Atmospheric and Space Physics,  
University of Colorado, Boulder, Colorado 80302*

K. E. SIMMONS AND L. K. McLAUGHLIN

*Laboratory for Atmospheric and Space Physics,  
University of Colorado, Boulder, Colorado 80302*

Received September 21, 1973

Ultraviolet spectrometer measurements of the reflectance at 3050 Å are modeled to give pressure-altitudes for Mars assuming a quiescent atmosphere. Ultraviolet light that is Rayleigh-scattered by the Mars molecular atmosphere, with allowance for uniform turbidity, is proportional to surface pressure independent of atmospheric temperature structure. All model constants except the over-all scaling factors are found by requiring ultraviolet spectrometer pressures of 47 locations on the planet to be the same when measured at different geometries. The overall scaling factor is found by intercomparison with Mariner 9 occultation pressures. Comparison with other Mars pressure-altitude measurements show deviations from the assumption of uniform turbidity to occur over the Hesperia plateau for ultraviolet measurements obtained during the 13-26 February 1972 time period.

### INTRODUCTION

Variations in the reflectance of Mars at 3050 Å are governed by local variations in the surface pressure, which are, in turn, controlled primarily by local surface topography (Barth and Hord, 1971; Hord, 1972; Hord *et al.*, 1972). Local surface pressure variations are equivalent to changes in the molecular column density. In the optically thin limit, changes in the molecular column density cause proportional changes in the intensity of the atmospheric scattered ultraviolet light. Reflectance at 3050 Å is a measure of surface pressure on Mars when the geometry of the measurement is corrected for and consideration is given to the effects of ground reflectance and turbidity. Radio occultation pressure measurements (Kliore *et al.*, 1972) are used for comparison to determine the absolute pressure scale.

The 3050 Å reflectance data analyzed in this work were obtained by the Mariner 9 ultraviolet spectrometer experiment dur-

ing the time period from January 23, 1972 to March 1, 1972. Each data point represents the average spectrometer intensity measured in a 100 Å band centered at 3050 Å. One measurement of this type was obtained every 3sec corresponding to an area  $10 \times 30$  km on the surface of Mars. When the Mariner 9 instruments were pointed in a fixed direction, the spacecraft motion caused the projected fields of view to sweep across the surface of Mars from southwest to northeast on the afternoon side of the planet. Data obtained during these mapping sequences provided a contiguous set of measurements along a smooth ground track which passed through the centers of the Mariner 9 television pictures obtained during the same data-taking sequence. A series of orbits of the Mariner 9 spacecraft provided a set of mapping swaths for all longitudes of the planet. Data obtained along these swaths, separated by 9° in longitude intervals, provide the basis for the present analysis.

Measurements were not included if the

geometry of observation was extreme, i.e., if the cosine of the solar incidence angle,  $\mu_0$ , or the cosine of the observing angle measured from the normal,  $\mu$ , were less than 0.3. Preliminary analysis has shown that data obtained for local times on the morning side of Mars do not correlate as well with the radio occultation pressures (Kliore *et al.*, 1972) as data obtained in the afternoon hours. For this reason, 3050 Å reflectance measurements made in the Martian morning are not used in this analysis. When rapid changes occurred in the scattering angle,  $\psi$ , due to spacecraft pointing movement, the measurements were not included. When the scattering angle was unchanged by spacecraft pointing motion, the data were included. Since the preliminary analysis of these data (Hord *et al.*, 1972), improvements in the spacecraft pointing information have led to more reliable ultraviolet pressure-altitude measurements. Eight spurious comparison points with the radio occultation experiment used in the preliminary analysis have been eliminated.

#### PRESSURE FORMULA

The approach adopted here is to find the simplest form for the conversion of 3050 Å reflectance,  $R$ , into surface pressure,  $P$ . Consideration of second order effects introduces additional parameters; these are later excluded from the pressure formulation if they do not significantly improve the predicted pressures. Two criteria have been used to assess the choice of parameters for the conversion of reflectance into surface pressure. First, the pressure formula should give the same value of pressure as the reflectance measurements at the same location on Mars, obtained at different geometries. Second, the conversion formula should produce the best possible agreement with pressures obtained by the radio occultation experiment (Kliore *et al.*, 1972; Kliore *et al.*, 1973).

Comparison points with the radio occultation experiment were selected by searching all ultraviolet measurements within 3°

of an occultation point in the latitude range 50°S to 40°N. Two sets of occultation measurements were included in this search; the standard mission occultations which occurred on orbits 1-79 and the extended mission occultations which occurred after orbit 352. Calculations for both sets of occultation pressures were carried out. Analysis showed that the extended mission data did not improve the values of the ultraviolet pressure coefficients sufficiently to be included in the analysis. A search of standard mission occultation measurements gave a total of 57 ultraviolet data tracks passing within 3° of 34 different occultation points. Several isolated comparison points were found where the spacecraft pointing motion swept the spectrometer field of view rapidly across an occultation location. These isolated points were not considered and are not included in the above number of comparison points.

Measurements obtained on closely adjacent ground tracks were used to form data pairs. Five measurements along each track were averaged to form a single point for comparison with the five-point average of the adjacent track, obtained with a different pointing geometry. In this way, a total of 47 comparison pairs were formed in order to test the self-consistency of the ultraviolet pressures. These comparison pairs occurred in three nearly equal groups at latitudes 30°S, 5°S, and 30°N.

A three-step procedure was adopted in order to determine the correct parameters in the formula for conversion of 3050 Å reflectance to surface pressure. First, parameters were determined independently from the 47 ultraviolet comparison pairs and from 57 ultraviolet radio occultation comparison points. Second, values of the parameters obtained by the two methods were checked for agreement, i.e., within the error estimates found in the two least squares adjustments. The third step in the procedure was to adopt the value of the parameter having the smallest standard error. According to this procedure, the formula relating the Mars reflectance at 3050 Å to the mole-

cular scattering optical depth,  $\tau_R$ , is

$$R = 1.25[p(\psi)\tau_R/4\mu] + 0.0156\mu_0, \quad (1)$$

where  $\tau_R$  is proportional to the surface pressure. A surface pressure of 6.0 mbar in a carbon dioxide atmosphere has a scattering optical thickness of 0.032. The first term in Eq. (1) is due to atmospheric scattering with an effective turbidity factor of 1.25. The second term represents the surface scattering contribution in the form of a Lambert surface with a coefficient 0.0156. Care should be exercised in attaching physical significance to the precise form and numerical coefficient values in Eq. (1). Errors of a few percent in the comparison pressures can lead to significant differences in the form of Eq. (1) found from least squares techniques. The Rayleigh scattering phase function is  $p(\psi) = 3/4 (1 + \cos^2\psi)$ . The ratio of the numerical coefficients in Eq. (1) was found by minimizing the root mean square error among the 47 ultraviolet comparison pairs. Ultraviolet pressures are reproduced by a second measurement to within 7%. The 57 radio occultation comparison points used to determine the normalization of the coefficients in Eq. (1) give pressures that agree with the radio occultation results with an error of about 12%. Table I shows a comparison of ultraviolet and occultation pressures at the 57 intercomparison points.

Figure 1 shows the aerographic location of the 3050 Å ultraviolet spectrometer reflectance measurements. The 47 ultraviolet intercomparison pairs are indicated by rectangular boxes, while the 34 occultation comparison points are designated by circles. Values of the ultraviolet pressure determined from 57, 3050 Å reflectance measurements within 3° of occultation comparison points are listed in Table 1. Figure 2 shows ultraviolet pressure plotted as a function of occultation pressure for the same 57 ultraviolet measurements. Figure 3 shows a comparison of the Mariner 9 infrared interferometer spectrometer pressures (Conrath *et al.*, 1973) with the ultraviolet pressures at the same locations on Mars. The Mariner 9 infrared pressures used in the comparison were from a table of values averaged over 5° in latitude and longitude supplied by Pearl (1973).

Altitude variations measured by earth-based radar (Downs *et al.*, 1973; Pettengill *et al.*, 1973) may be compared with ultraviolet pressure-altitude measurements with a satisfactory conversion from altitude to local surface pressure. Pressure varies with location on the Martian surface due to deviations in the equipotential surface, or geoid, from spherical symmetry (Lorell *et al.*, 1973; Cain *et al.*, 1973). In addition, pressures may differ from those expected from the simple geoid model, due to

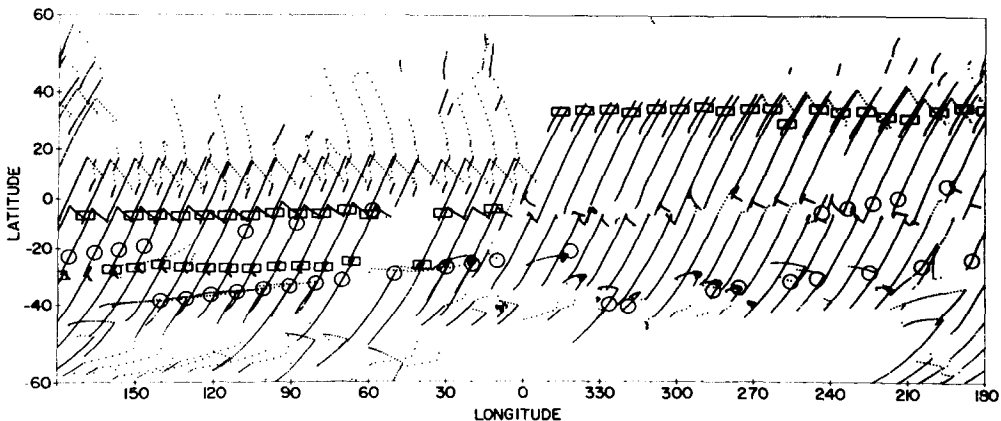


FIG. 1. Location of ultraviolet measurements used in this analysis. Rectangular boxes show location of ultraviolet intercomparison pairs and circles show location of radio occultation comparison measurements.

TABLE I.

## Mariner 9 Pressure Comparison

P(UV)	P(OCC)	Diff.	UV Orbit	OCC Orbit	Lat.	Lon.	Location
5.6	4.3	1.3	140	29	-26.4	204.3	M. Cimmerium
4.3	4.9	-0.6	140	33	-23.9	185.1	Rasena
4.4	4.4	0.0	142	35	-23.0	175.5	Atlantis
4.2	4.4	-0.2	144	37	-21.6	165.3	M. Sirenum
4.1	4.9	-0.8	146	39	-20.7	155.8	Memnonia
4.0	4.5	-0.5	148	41	-19.2	146.0	Memnonia
4.3	4.3	0.0	150	2	-40.5	142.5	M. Sirenum
4.9	4.4	0.5	150	6	-38.4	141.0	M. Sirenum
4.4	4.4	0.0	152	6	-38.8	140.4	M. Sirenum
4.2	4.3	-0.1	152	2	-38.9	143.2	M. Sirenum
3.8	4.3	-0.5	154	2	-39.9	142.6	M. Sirenum
4.3	3.5	0.8	156	8	-37.4	130.4	Serenum S.
5.2	4.1	1.1	156	10	-37.0	120.2	Icaria
2.7	2.9	-0.2	156	49	-13.4	107.8	Phoenicis L.
4.8	3.6	1.2	158	12	-35.7	110.9	Daedalia
3.7	2.8	0.9	160	14	-35.0	101.4	Claritas
4.1	3.6	0.5	160	12	-35.4	110.4	Daedalia
3.6	2.8	0.8	160	14	-34.6	100.2	Claritas
3.0	3.4	-0.4	160	53	- 9.8	88.1	Tithonius L.
3.3	3.4	-0.1	162	16	-33.8	90.4	Solis Lacus
4.1	3.5	0.6	164	18	-32.5	80.3	Solis Lacus
3.4	3.4	-0.0	164	16	-33.2	90.9	Solis Lacus
2.8	2.8	-0.0	164	14	-33.7	100.9	Claritas
3.9	3.5	0.4	164	18	-32.5	80.2	Solis Lacus
3.5	3.8	-0.3	166	20	-31.6	70.4	Thaumasia
4.6	4.2	0.4	166	59	- 4.5	58.2	Juventae Fons
5.0	4.7	0.3	170	24	-29.3	49.9	M. Erythraeum
5.6	4.9	0.7	174	28	-27.1	29.4	Pyrrhae R.
5.6	4.9	0.7	174	28	-26.9	29.6	Pyrrhae R.
5.7	4.9	0.8	174	28	-27.0	30.4	Pyrrhae R.
5.4	5.5	-0.1	176	30	-25.9	19.6	Pyrrhae R.
5.3	5.5	-0.2	178	30	-25.7	19.8	Pyrrhae R.
5.2	5.5	-0.3	178	30	-26.1	19.7	Pyrrhae R.
5.0	5.5	-0.5	178	30	-25.7	19.8	Pyrrhae R.
5.9	5.5	0.4	182	30	-25.7	20.3	Pyrrhae R.
5.5	5.5	0.0	182	30	-25.4	19.8	Pyrrhae R.
5.4	5.5	-0.1	182	30	-26.2	19.6	Pyrrhae R.
5.2	5.5	-0.3	182	30	-25.1	19.9	Pyrrhae R.
5.0	4.9	0.1	184	32	-23.1	11.1	Pyrrhae R.
3.8	4.6	-0.8	186	38	-22.6	342.4	Pandorae Fr.
3.8	4.4	-0.6	190	3	-39.4	326.5	Hellespontus
4.1	4.4	-0.3	192	3	-39.8	326.4	Hellespontus
4.4	4.7	-0.3	194	1	-40.1	318.9	Yaonis Regio
8.2	8.7	-0.5	200	13	-35.6	285.2	Hellas
7.3	8.7	-1.4	200	13	-34.3	286.3	Hellas
7.0	6.8	0.2	202	15	-34.6	276.2	M. Hadriacum
6.8	6.8	-0.0	202	15	-34.0	275.8	M. Hadriacum
6.3	6.8	-0.5	202	15	-33.7	275.6	M. Hadriacum
6.9	6.8	0.1	202	15	-34.4	276.0	M. Hadriacum
5.3	5.0	0.3	204	58	- 5.0	244.4	Tritonis S.
5.8	4.6	1.2	206	60	- 3.6	234.3	Gomer
4.3	4.7	-0.4	208	21	-31.8	243.7	M. Tyrrhenum
5.6	4.6	1.0	208	19	-31.9	255.9	Ausonia
5.4	6.3	-0.9	208	62	- 1.6	224.1	Aeolis
5.3	6.4	-1.1	210	64	0.3	213.9	Aeolis
4.5	4.3	0.2	212	25	-28.0	224.4	Hesperia
6.2	7.1	-0.9	214	68	4.7	193.4	Mesogaea

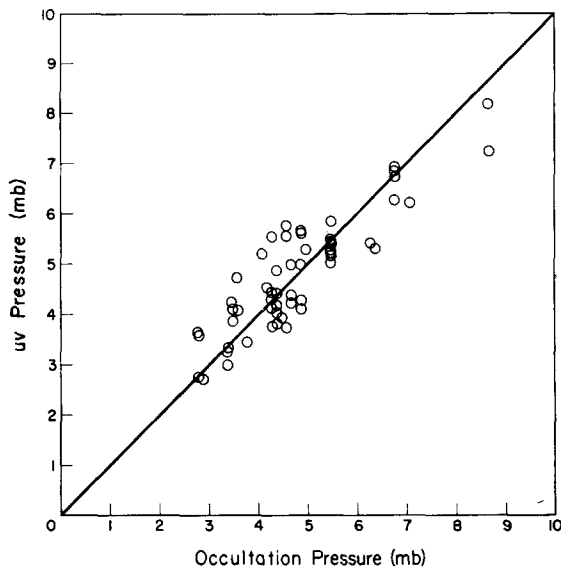


FIG. 2. Comparison of ultraviolet pressures with the radio occultation experiment.

atmospheric effects. Models of the Martian circulation (Leovy and Mintz, 1969; Conrath *et al.*, 1973) indicate that differences may be expected as a function of latitude, season, and time of day. Long time scale episodic variations in pressure may occur (Sagan, 1973). In Fig. 4, a simple barometric transformation has been used in order to compare ultraviolet pressures with the 1971 earth-based radar measure-

ments of Pettengill *et al.* (1973). Conversion of radar altitudes to effective pressures was accomplished by choosing an isothermal scale height of 12 km and adjusting the radar altitude zero to the triple point pressure of water, 6.1 mbar (Hord, 1972). Assuming a scale height smaller than 12 km worsened the correlation between ultraviolet and radar data. Occultation temperature profiles indicate that the

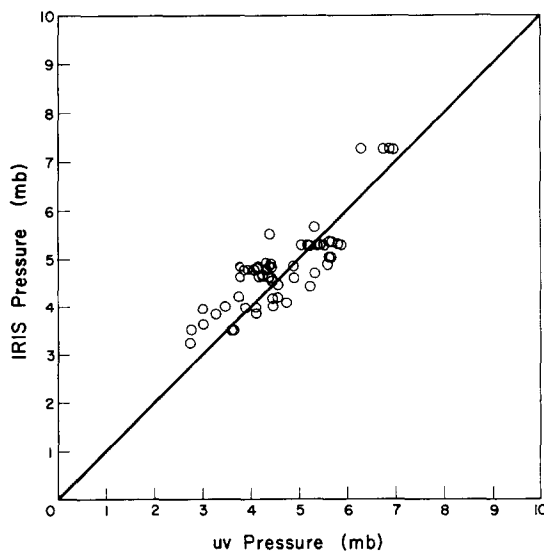


FIG. 3. Comparison of Mariner 9 infrared pressures with ultraviolet pressures.

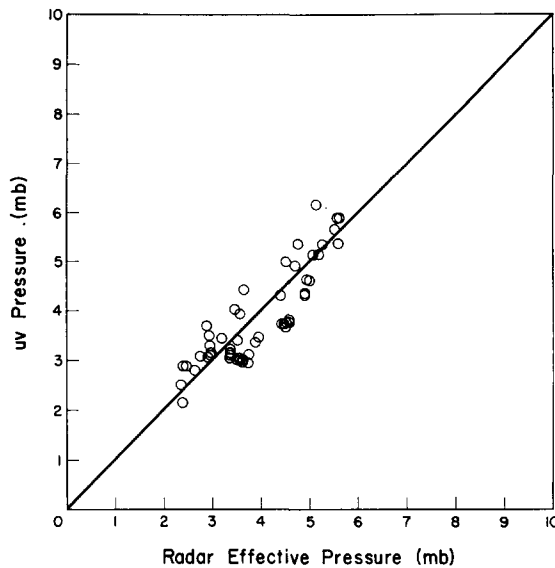


FIG. 4. Comparison of ultraviolet pressure with earth-based radar measurements. Radar topography is expressed as an effective pressure, assuming an isothermal atmosphere.

12km scale height is reasonable for the midafternoon (Kliore, 1973) for ultraviolet reflectance measurements made at  $15^\circ$  south latitude (the location of the 1971 radar measurements). The effect of the gravity anomaly centered in the Tharsis region (Lorrell *et al.*, 1973) is strongly correlated with the selection of a scale height as the highest altitudes also occur in Tharsis. For this reason, the systematic effect of gravity may be partially compensated by the selected scale height. More complicated temperature structure models for conversion of pressure to altitude were not found to significantly improve the correlation seen in Fig. 4. Radar comparison points in the longitude range from  $210^\circ$  to  $270^\circ$  have been excluded from Fig. 4. Atmospheric dust is believed to affect the ultraviolet pressures in this region.

#### SECONDARY EFFECTS

In all of the comparisons discussed in the previous section, the regions of Mars sampled by the several measurement methods differed in effective area sampled on the planet surface. These differences undoubtedly account for some of the

differences in pressures shown in Figs. 2, 3, and 4. Occultation pressures may be expected to be systematically lower than those determined by other methods: the highest local topographic feature will occult the radio signal so that the measured pressure will be characteristic of that topographic height. Since the ultraviolet pressure measurements are normalized to radio occultation pressures, there should be a small systematic lowering of the ultraviolet pressures compared with those measured by the Mariner 9 infrared interferometer spectrometer experiment. Seasonal and time of day pressure effects could contribute to the differences in the intercomparison of ultraviolet and occultation pressures. Infrared and ultraviolet measurements were made simultaneously so that seasonal and time of day pressure variations were eliminated. Differences in the ultraviolet and infrared measurements occur because of the much higher spatial resolution of the ultraviolet instrument ( $10 \times 30$  km) compared with the infrared instrument ( $125 \times 125$  km). Comparison of ultraviolet pressures with radar topographic altitudes are also influenced by differing sampling areas as well as gravity and atmospheric pressure models referred

to earlier. The effective sampling area of the Goldstone radar measurements is  $8 \times 80$  km with the long dimension along a meridian (Downs *et al.*, 1973). Radar measurements by the Haystack group sampled an area  $100 \text{ km}^2$  (Pettengill *et al.*, 1973).

More complicated equations for the conversion of ultraviolet reflectance to surface pressure have been tested. Equation (2) includes the effects of scattering and extinction for molecules and dust and allows for a Minnaert representation of surface scattering:

$$R = \left[ \frac{p(\psi)\tau_R + p_d(\psi)\bar{\omega}_d\tau_d}{4\mu} \right] \left[ \frac{1 - \exp(-\tau m)}{\tau m} \right] + R_0 \frac{(\mu\mu_0)^k}{\mu} \exp(-\tau m). \quad (2)$$

The effect of dust scattering is represented by the product of the dust phase function,  $p_d(\psi)$ ; single scattering albedo,  $\bar{\omega}_d$ ; and optical thickness,  $\tau_d$ . Extinction depends upon the product of total optical depth,  $\tau = \tau_R + \tau_d$ , and airmass,  $m = 1/\mu + 1/\mu_0$ . The Minnaert coefficients,  $R_0$  and  $k$ , may also be functions of the scattering angle,  $\psi$ .

Using nonlinear least squares techniques, the parameters in Eq. (2) were varied in order to minimize errors in comparison with the radio occultation comparison points. Using this criterion, a statistically significant improvement was not found. In these regressions two types of dust distributions were used. One type assumed uniform turbidity with  $\tau_d$  proportional to  $\tau_R$ . A second type assumed a constant amount of dust above the surface,  $\tau_d = \text{constant}$ .

If the probable error in the radio occultation pressures is about 5% (Kliore, 1973), this in itself is sufficient to preclude obtaining definitive values for the coefficients in Eq. (2). The systematic manner of the accumulation of ultraviolet data, evident in Fig. 1, causes some effects to be highly correlated and, therefore, difficult to separate. An example of this effect is the correlation between the choice of surface scattering parameter,  $k$ , and dust extinction optical thickness,  $\tau_d$ .

If  $k$  is reduced from a value of unity used in Eq. (1) to 0.4, then dust extinction may be included, using Eq. (2), without any material change in the agreement of ultraviolet and occultation pressures. Equation (1) should be thought of as one in a family of possible equations giving the surface pressure on Mars.

A number of effects become important if pressures are to be improved and the error reduced below the 5% level. Variability in ultraviolet surface albedo, multiple scattering effects, field of view differences, local variations in turbidity, and the high altitude scattering layer (e.g., Ajello *et al.*, 1973; Ajello and Hord, 1973) are a few of these effects.

Extreme geometries provide more specific atmospheric and surface scattering parameters than surface pressure predictions described in this paper. Extreme geometries are those with  $\mu$  or  $\mu_0$  less than 0.3 or with a more extended range of the scattering angle,  $\psi$ . Comparison of the ultraviolet measurements with those of the Mariner infrared interferometer spectrometer will give additional long wavelength information to find these parameters.

Over the major part of the planet, Eq. (1) converts ultraviolet reflectance into pressure-altitudes in agreement with other measurements with a standard error of less than 1 km in altitude. Comparisons of other pressure and altitude measurements produce comparable results.

#### ATMOSPHERIC DUST

A notable exception to the general agreement of ultraviolet measurements with other data occurred in one area of the planet. Figure 5 shows the comparison of all ultraviolet measurements within  $3^\circ$  of the 1971 Haystack radar facility measurements (Pettengill *et al.*, 1973). Measurements from  $210$  to  $270$  degrees longitude, around Hesperia, are included as well as the measurements shown in Fig. 4. Most of the disagreement is confined to this specific area of Mars. Other comparisons with Mariner 9 occultation and infrared spectrometer measurements confirm this deviation in the ultraviolet. The

ultraviolet data over this region were obtained during the 13–26 February 1972 time period, well after the major dust storm had settled.

A number of hypotheses could explain the apparent high pressures in the ultraviolet. An increase in the ultraviolet surface scattering albedo over this longitude range seems unlikely. Soderblum (1973) pointed out that the high plateau around Hesperia is the smoothest region on the planet and could lead to a stable circulation pattern accompanied by an ultraviolet haze. However, no systematic scattering layer is observed over Hesperia (Ajello *et al.*, 1973; Ajello and Hord, 1973).

The most likely explanation is that a large scale change in atmospheric turbidity occurred in the Hesperia region while ultraviolet measurements were being made. Under this assumption, the atmosphere at the time of the Hesperia observations had a turbidity between dust storm and clear conditions. During the dust storm observations, beginning on November 14, 1971, the single scattering albedo of the dust particles was found to be  $\tilde{\omega}_d = 0.18$  if  $\tau_d = 1$ , or  $\tilde{\omega}_d = 0.20$  if  $\tau_d = \infty$  (Barth *et al.*, 1972; Hord *et al.*, 1972). If  $\tilde{\omega}_d \approx 0.2$  is a reasonable value for the dust

particles remaining in the atmosphere after the dust storm subsided, then, by using Eq. (2), an estimate can be made of the residual dust opacity during the clear period when ultraviolet pressures were obtained. For clear period data, excluding the Hesperia region, the dust opacity was  $\tau_d = 0.05$ – $0.10$ . The dust optical thickness is not well specified, since variations in turbidity for values less than 0.1 produce a small effect on the ultraviolet pressure. Increasing the dust optical thickness tends to increase the observed brightness because of the added scattering from dust particles. The dust, in addition to scattering, is also absorbing, and this absorption reduces the brightness from the molecular atmosphere. Scattering and absorption effects are nearly equal for the value of  $\tilde{\omega}_d = 0.2$ . The net effect is a weak dependence upon the dust mixing ratio. For the Hesperia region, the observed differences in effective ultraviolet pressure could be accounted for if the dust opacity is larger,  $\tau_d > 0.3$ . Television pictures obtained at the time of the ultraviolet measurements show considerably less detail than others obtained of the same region later in the mission (Masursky, 1972). This lack of detail in the earlier set of pictures indicates

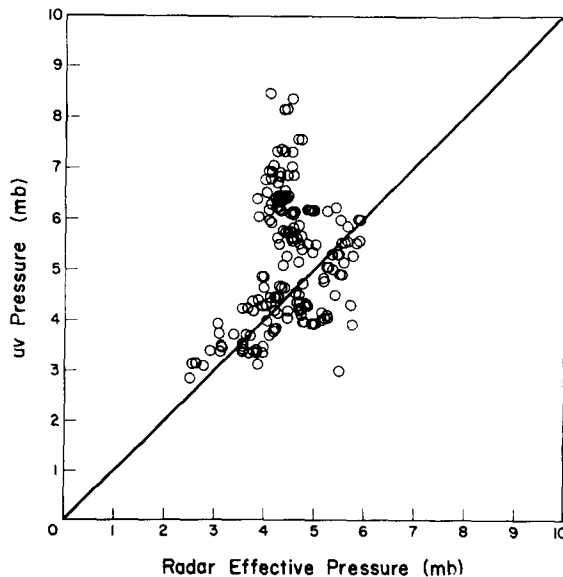


FIG. 5. Comparison of ultraviolet pressure with effective radar pressure including measurement in Hesperia.

an increase in atmospheric turbidity over Hesperia. Also the apparent high ultraviolet pressures over this region are similar to earthbased measurements of CO<sub>2</sub> abundance at a wavelength of 1  $\mu$ m during the dust storm (Parkinson and Hunten, 1973).

#### PRESSURE-ALTITUDES

Figure 6 shows the ultraviolet pressure-altitude contours at one-kilometer intervals. A 12-km scale height was used to convert pressure to altitude. Zero altitude corresponds to a surface pressure of 6.1 mbar. The background Mercator map was made from Mariner 9 television pictures (U.S. Geological Survey, 1972). The region from 210° to 270° longitude with a large amount of dust in the atmosphere at the time of the measurements has not been contoured.

The highest feature on the planet measured in the ultraviolet is the volcano Olympus Mons (Nix Olympica). Three different paths of the ultraviolet spectrometer projected field of view passed close to the volcano summit. Since the slope of the volcano is large, a correction was made for the effect of local slope on the surface scattering subtraction. The procedure used was, first, to calculate an altitude profile using Eq. (1) and, second, to use the determined altitude profile along with knowledge of the solar direction to recalculate the effective solar illumination and emission angles used in finding the surface-scattering term. This procedure was iterated to convergence. A correction for the high altitude scattering layer (Leovy *et al.*, 1972; Ajello *et al.*, 1973) was included in this calculation. Since none of the ultraviolet profiles crossed the volcano summit, each of the 3 altitude profiles was extrapolated to the edge of the summit caldera as determined from television pictures. By the method described, the summit is found to occur 25 km above the surrounding region or at an altitude of 29 km above the 6.1 mbar pressure level. The triaxial ellipsoid representation of the 6.1 mbar equipotential surface from the radio occultation experi-

ment gives a radius of 3392.5 km at Olympus Mons (Cain *et al.*, 1973), leading to an areocentric radius of 3421.5 km at the top of the volcano. Determinations using geometric or photogrammetric methods applied to Mariner 9 television pictures are in substantial agreement with the ultraviolet measurement (Davies, 1973; Wu *et al.*, 1973; Blasius, 1973).

Figure 7 shows the ultraviolet contour map overlaid on a Mariner 9 planning map prepared by de Vaucouleurs. It is notable that the ultraviolet contours are not related to the visual albedo markings, shown in light and dark tones. The ultraviolet altitude corresponds to brightness at 3050 Å: the lower altitudes are brighter.

The effect of the 1971 dust storm on ultraviolet intensity was a loss of contrast rather than a general change in the planet-wide brightness. Small differences in the Mariner 9 and Mariner 6 and 7 calibrations gave the early impression that the brightness level was less during the 1971 dust storm than under clear conditions in 1969, when Mariner 6 and 7 observations were made (Barth *et al.*, 1972). The loss of contrast means that the apparent pressure-altitude of a high region appears lower, e.g., Tharsis, and a low region appears higher, e.g., Hellas. As dust is introduced into the atmosphere, the dust particle single scattering albedo,  $\tilde{\omega}_d$ , of order 0.2, leads to a loss of contrast in the ultraviolet. If  $\tilde{\omega}_d$  were larger, the whole planet albedo would increase during a dust storm. In Figs. 6 and 7, the apparent depth of Hellas is less than 3 km compared with a depth of about 4 km measured by the radio occultation experiment. This difference supports the idea that atmospheric dust remains in Hellas, while the rest of the planet is clear (e.g., Parkinson and Hunten, 1972).

A detailed presentation of the ultraviolet topographic profiles shown with television pictures is in preparation. This Mariner 9 ultraviolet spectrometer data report will be available shortly from the Laboratory for Atmospheric and Space Physics at the University of Colorado. The maximum spatial resolution, 10  $\times$  30 km, is used in these data. An example of a

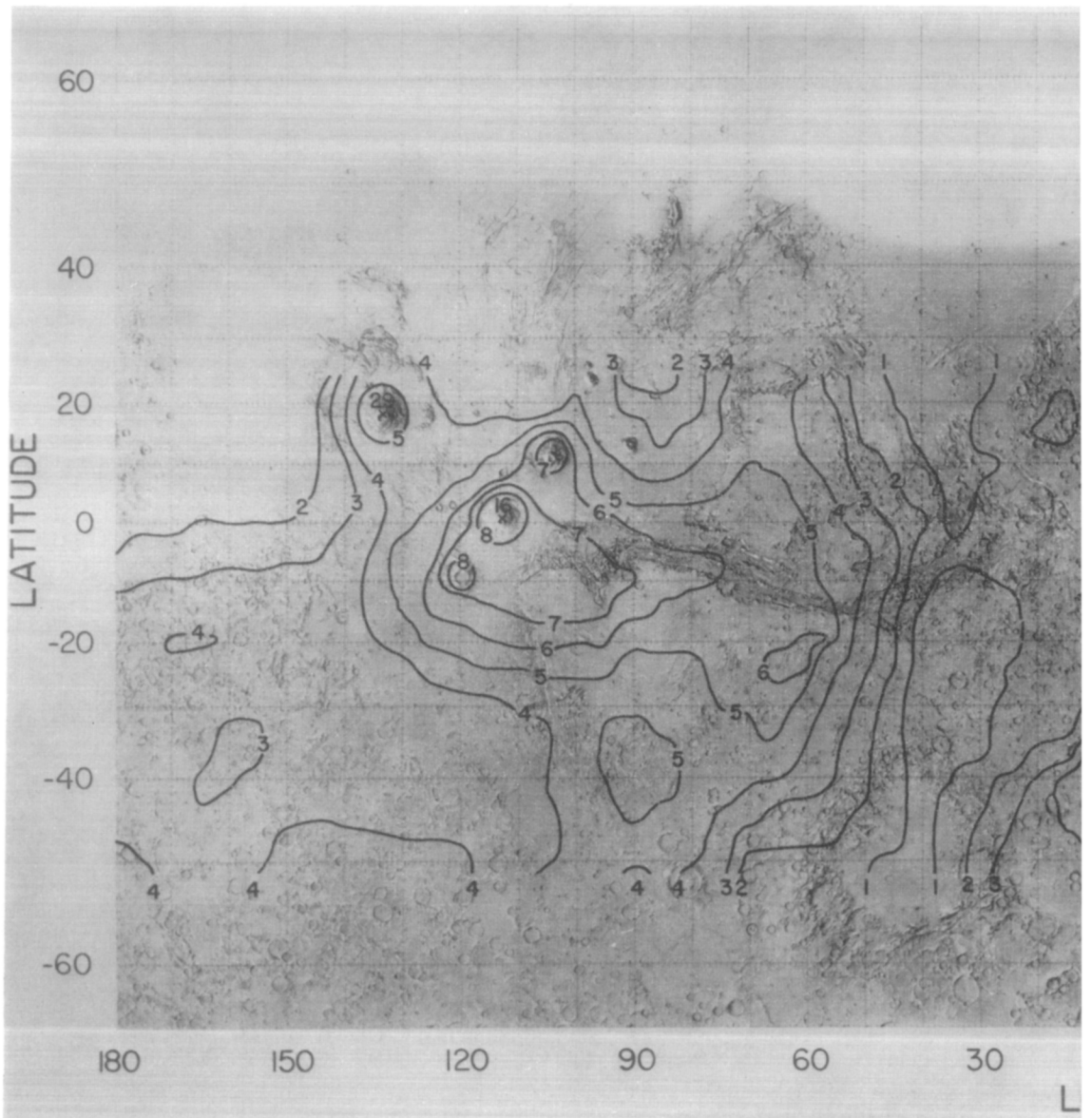
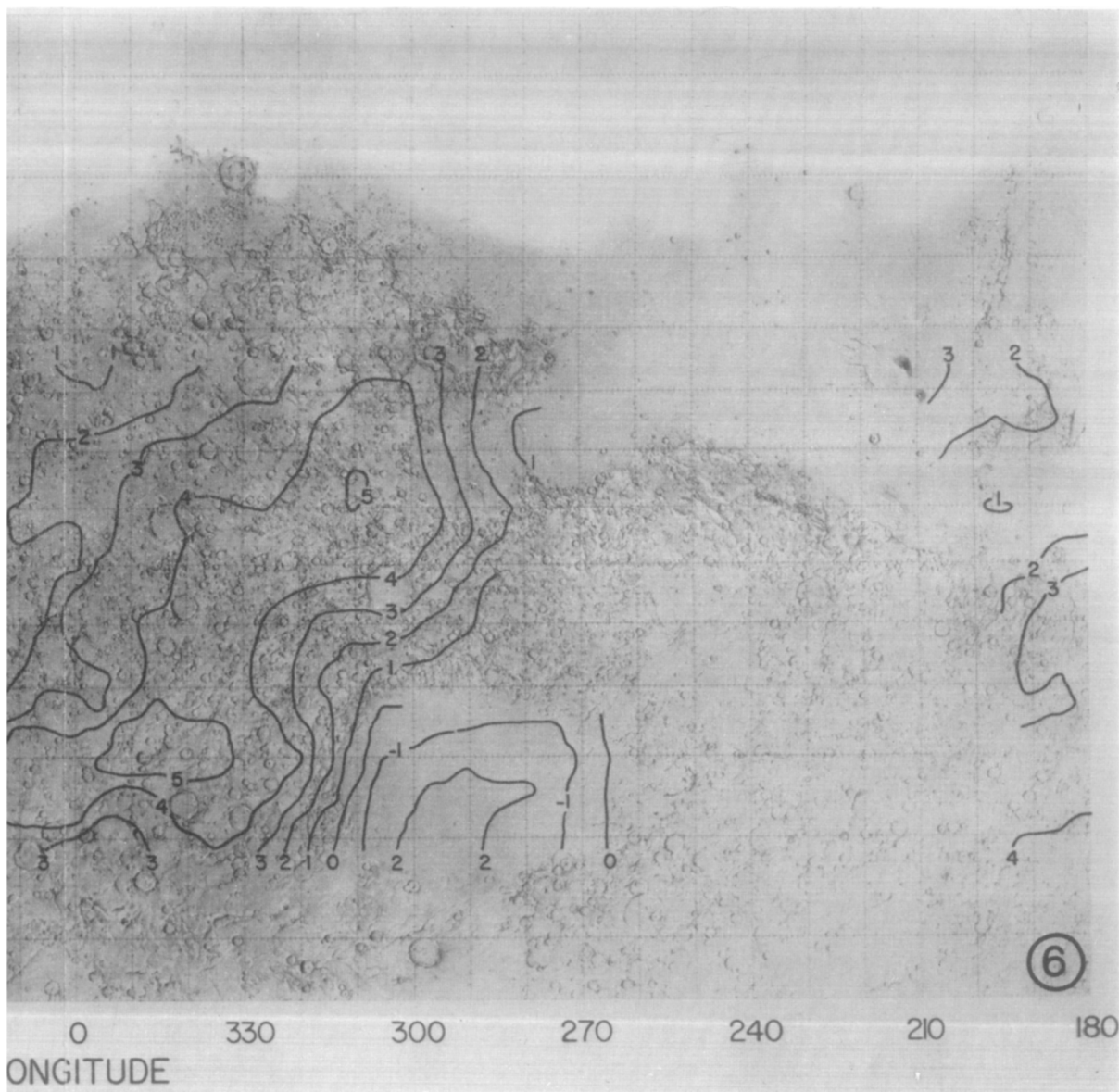


FIG. 6. Ultraviolet pressure-altitude contour map of Mars. The measurements have been smoothed to The region from longitude 210° and 270° was dusty at the time the measurements were made. The back



10° in longitude and latitude except for the volcanos Middle Spot and Nix Olympica, where more detail is shown. ground map, made from Mariner 9 television pictures, was provided by H. M. Masursky.

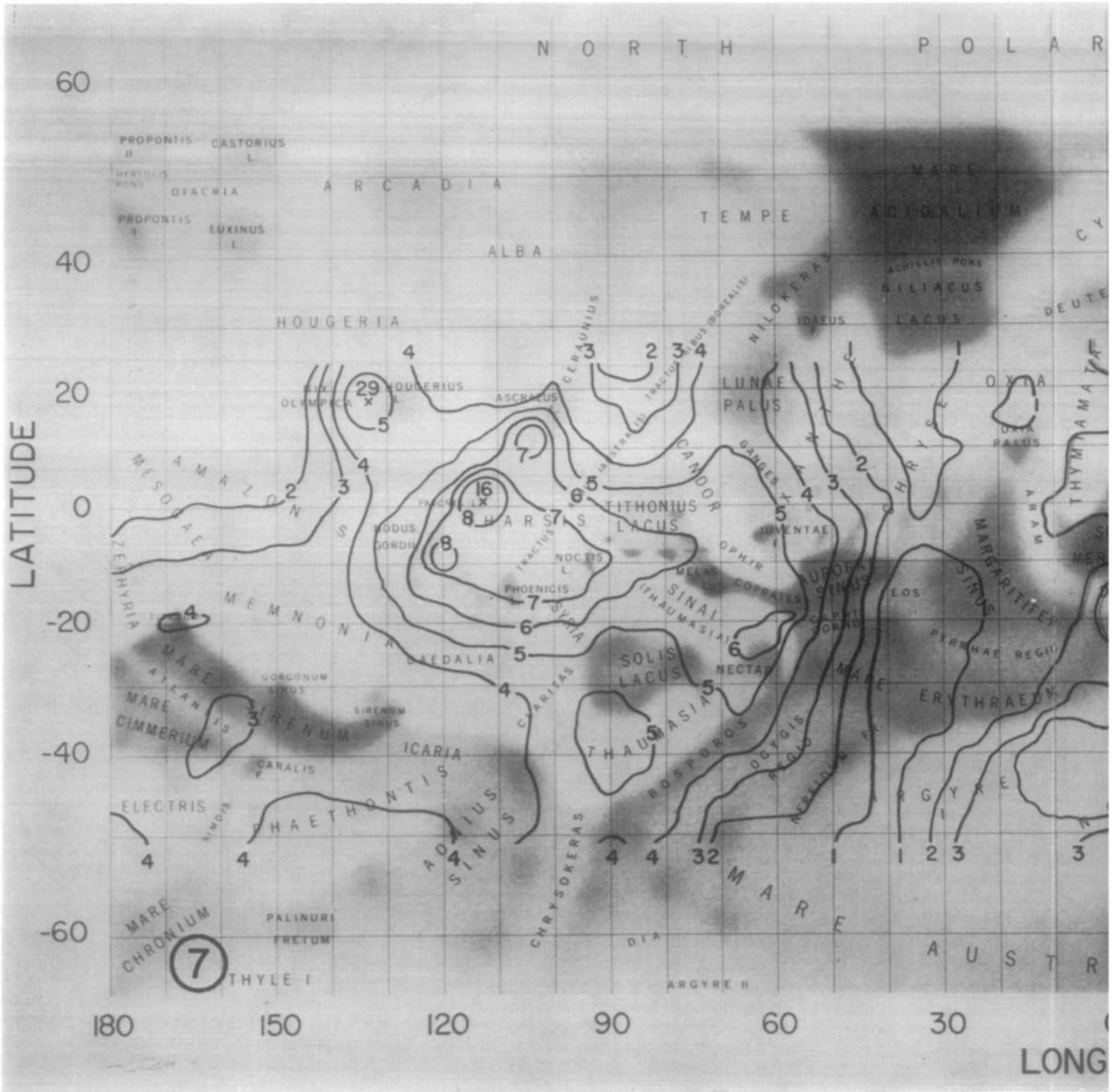
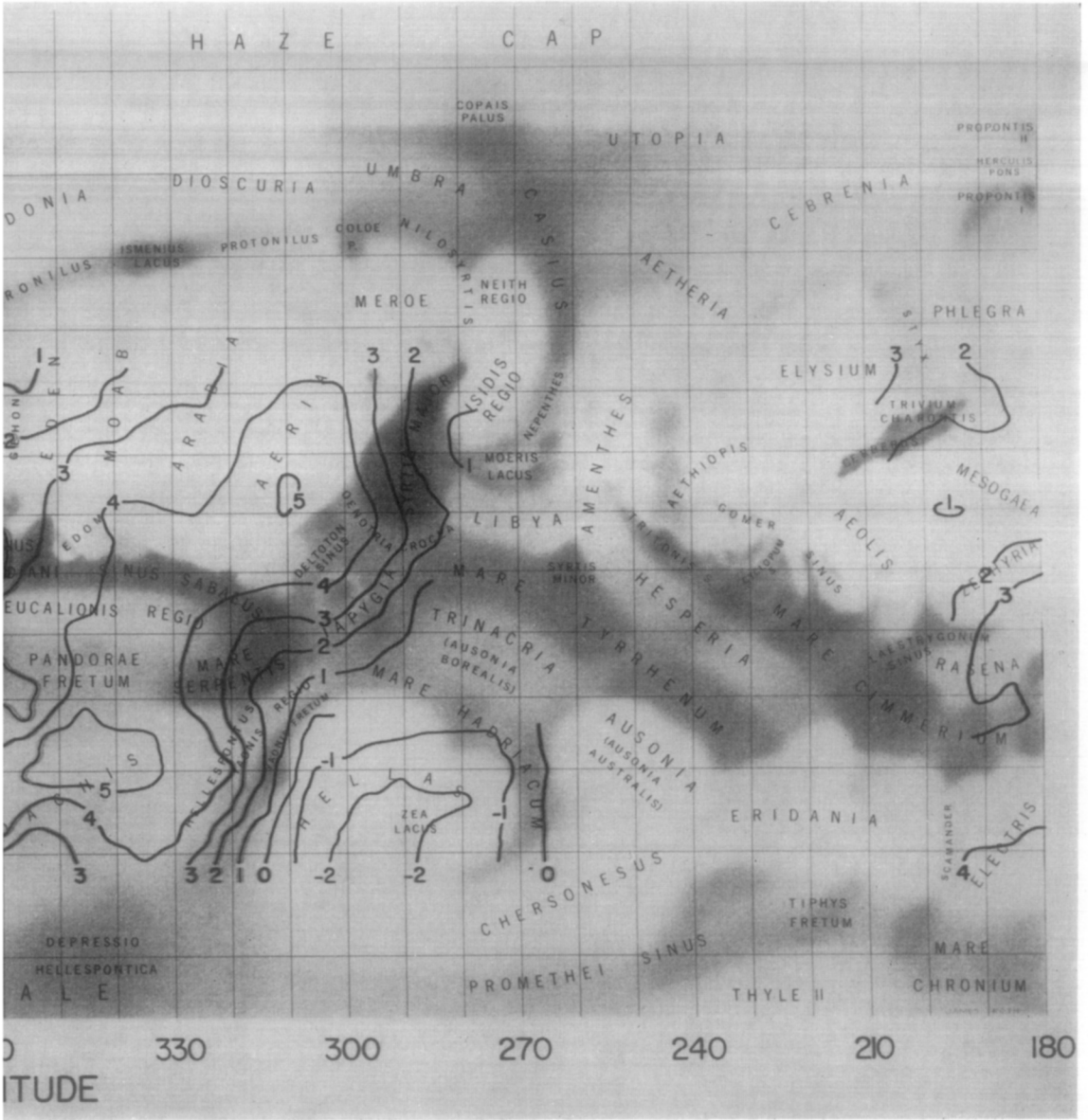


FIG. 7. Ultraviolet pressure-altitude contour map of Mars overlaid



on a Mariner 9 planning map prepared by G. de Vaucouleurs.

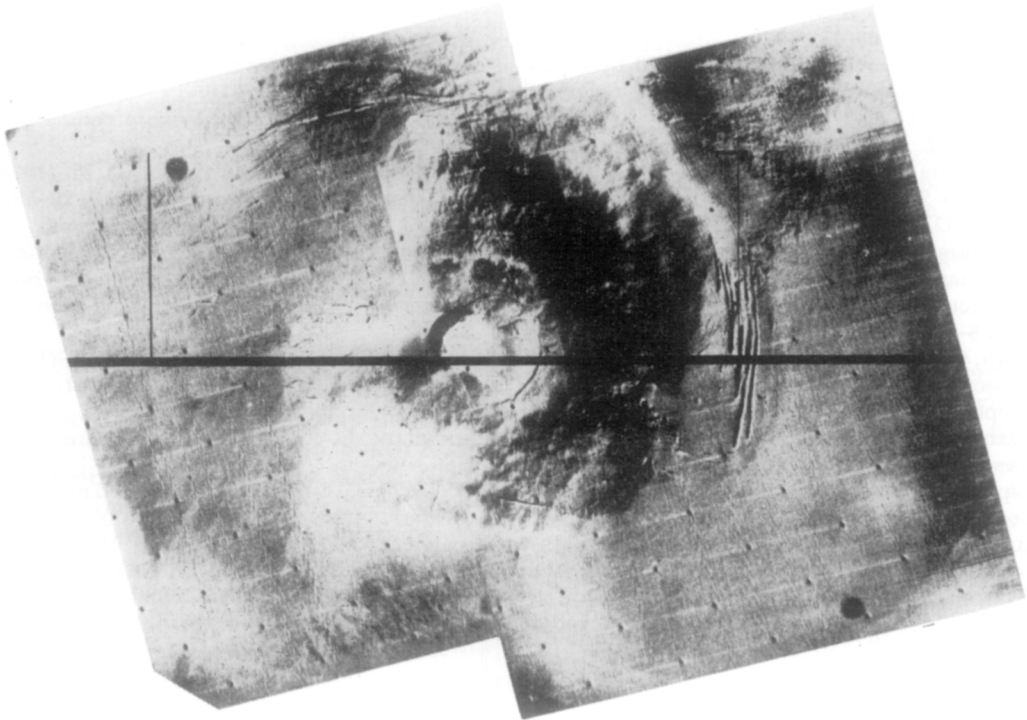
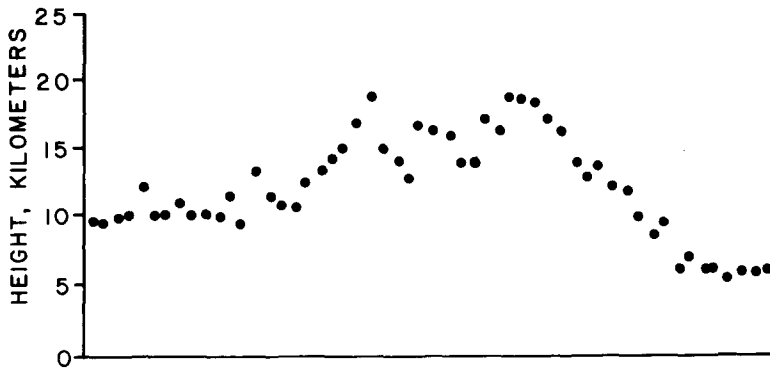


FIG. 8. Ultraviolet pressure-altitude profile across the volcano Middle Spot. The local slope has been taken into account in computing the surface scattering effect used to find local pressure.

detailed ultraviolet topographic profile of the volcano Middle Spot is shown in Fig. 8.

#### ACKNOWLEDGMENTS

We thank Charles A. Barth for his valuable suggestions and assistance in doing this work. This work was supported by the National Aeronautics and Space Administration.

#### REFERENCES

- AJELLO, J. M., HORD, C. W., BARTH, C. A., STEWART, A. I., AND LANE, A. L. (1973). Mariner 9 ultraviolet experiment: Afternoon terminator observations of Mars. *J. Geophys. Res.* **78**, 4279-4290.
- AJELLO, J. M., AND HORD, C. W. (1973). Mariner 9 ultraviolet spectrometer experiment: Morning terminator observations of Mars. *J. Atmos. Sci.* **30**, 1495-1501.

- BARTH, C. A., AND HORD, C. W. (1971). Mariner ultraviolet spectrometer: Topography and polar cap. *Science* **173**, 197-201.
- BARTH, C. A., HORD, C. W., STEWART, A. I., AND LANE, A. L. (1972). Mariner 9 ultraviolet spectrometer experiment: Initial report. *Science* **175**, 309-312.
- BLASIUS, K. R. (1973). A study of Martian topography by analytic photogrammetry. *J. Geophys. Res.* **78**, 4411-4423.
- CAIN, D. L., KLIORRE, A. J., SEIDEL, B. L., SYKES, M. J., AND WOICESHYN, P. (1973). Approximations to the mean surface of Mars and Mars atmosphere using Mariner 9 occultations. *J. Geophys. Res.* **78**, 4352-4354.
- CONRATH, B., CURRAN, R., HANEL, R., KUNDE, V., MAGUIRE, W., PEARL, J., PIRRAGLIA, J., AND WELKER, J. (1973). Atmospheric and surface properties of Mars obtained by infrared spectroscopy on Mariner 9. *J. Geophys. Res.* **78**, 4267-4278.
- DAVIES, M. E. (1973). Photogrammetric measurements of Olympus Mons on Mars. *Icarus* **21**, 230-236.
- DOWNS, G. S., GOLDSTEIN, R. M., GREEN, R. R., MORRIS, G. A., AND REICHLEY, P. E. (1973). Martian topography and surface properties as seen by radar: The 1971 opposition. *Icarus* **18**, 8-21.
- HORD, C. W. (1972). Mariner 6 and 7 ultraviolet spectrometer experiment: Photometry and topography of Mars. *Icarus* **16**, 253-280.
- HORD, C. W., BARTH, C. A., STEWART, A. I., AND LANE, A. L. (1972). Mariner 9 ultraviolet spectrometer experiment: Photometry and topography of Mars. *Icarus* **17**, 443-456.
- KLIORRE, A. J. (1973). Private communication.
- KLIORRE, A. J., CAIN, D. L., FJELDBO, G., SEIDEL, B. L., AND SYKES, M. J. (1972). The atmosphere of Mars from Mariner 9 radio occultation measurements. *Icarus* **17**, 484-516.
- KLIORRE, A. J., FJELDBO, G., SEIDEL, B. L., SYKES, M. J., AND WOICESHYN, P. M. (1973). S band radio occultation measurements of the atmosphere and topography of Mars with Mariner 9: Extended mission coverage of polar and intermediate latitudes. *J. Geophys. Res.* **78**, 4331-4351.
- LEOVY, C., AND MINTZ, Y. (1969). Numerical simulation of the atmospheric circulation and climate of Mars. *J. Atmos. Sci.* **26**, 1167.
- LEOVY, C. B., BRIGGS, G. A., YOUNG, A. T., SMITH, B. A., POLLACK, J. B., SHIPLEY, E. N., AND WILDEY, R. L. (1972). The Martian atmosphere: Mariner 9 television experiment progress report. *Icarus* **17**, 373-393.
- LORELL, J., BORN, G. H., CHRISTENSEN, E. J., ESPOSITO, P. B., JORDAN, J. F., LAING, P. A., SJOGREN, W. L., AND WONG, S. K. (1973). Gravity field of Mars from Mariner 9 tracking data. *Icarus* **18**, 304-316.
- MASURSKY, H. M. (1972). Private communication.
- PARKINSON, T. D., AND HUNTEN, D. M. (1973). CO<sub>2</sub> distribution on Mars. *Icarus* **18**, 29-53.
- PEARL, J. (1973). Private communication.
- PETTENGILL, G. H., SHAPIRO, I. I., AND ROGERS, A. E. E. (1973). Topography and radar scattering properties of Mars. *Icarus* **18**, 22-28.
- SAGAN, C., TOON, O. B., GIERASCH, P. J. (1973). Climatic change on Mars. *Science* **181**, 1045-1048.
- SODERBLOM, L. A. (1973). Private communication.
- U.S. Geological Survey (1972). Shaded relief map of Mars, *Atlas of Mars*, MM 25 MIR I 810, scale 1: 25,000,000, Washington, DC.
- WU, S. S. C., SCHAFER, F. J., NAKATA, G. M., AND JORDAN, R. (1973). Photogrammetric evaluation of Mariner 9 photography. *J. Geophys. Res.* **78**, 4405-4410.